Chemical Science

This article can be cited before page numbers have been issued, to do this please use: S. K. Mandal, G. Vijaykumar, A. Pariyar, J. Ahmed, B. Shaw and D. Adhikari, *Chem. Sci.*, 2018, DOI: 10.1039/C7SC04687A.

View Article Online
DOI: 10.1039/C7SC04687A

Journal Name

ARTICLE

Tuning redox non-innocence of phenalenyl ligand toward efficient nickel-assisted catalytic hydrosilylation

Received 00th January 20xx,
Accepted 00th January 20xx

DOI: 10.1039/x0xx00000x

www.rsc.org/

Gonela Vijaykumar,[a] Anand Pariyar,[a] Jasimuddin Ahmed,[a] Bikash Kumar Shaw,[a] Debashis Adhikari,*[b] Swadhin K. Mandal*[a]

In this report, ligand-redox assisted catalytic hydrosilylation has been investigated. A phenalenyl ligand coordinated nickel complex has been utilized as an electron reservoir to develop a base metal assisted catalyst, which works very efficiently to hydrosilylate a wide variety of olefin substrates under ambient conditions. The mechanistic investigation unravels that a two-electron reduced phenalenyl based bi-radical nickel complex plays the key role in such catalysis. The electronic structure of the catalytically active biradical species has been interrogated by EPR spectroscopy, magnetic suceptibility measurement and electronic structure calculations by DFT method. The reaction inhibition by a radical quencher as well as mass spectrometric detection of two intermediates along the catalytic loop suggest that a single electron transfer from the ligand backbone initiates the catalysis. Such a strategy, leveraging the redox reservoir property of the ligand ensures that the nickel is not promoted to an unfavorable oxidation state, but the fine tuning between ligand and metal redox orbitals elicit smooth catalysis.

Introduction

Recently, the base metal catalysts have garnered tremendous verve and gusto since these can be ideal surrogate for scarce, expensive and often toxic 4d and 5d late transition metals.[1] Current strong interest in developing the base metal catalysts necessitates taming the metal to execute two-electron chemistry where the metal is usually prone to perform one-electron redox reactions. The co-operative action of the ancillary ligand along with the coordinated 3d metal might be an effective strategy to facilitate such a desirable multi-electron redox reaction onto it.[2] Executing co-operative catalysis between the base metal and ligand is probable if the later behaves as a reservoir for the redox equivalent. Appropriate redox tuning between the ligands and metal center can facilitate the redox chemistry without promoting the metal to an unusual and unfavorable oxidation state, which generally slows down the catalytic process. Seminal work from Chirik, Heyduk, Abu-Omar and Soper have showcased that metal-centric two electron chemistry is viable when the redox non-innocent ligands are electronically tuned with the metals.[3,4,5] As an alternative to ligand assisted metal-centered two-electron redox, it can also be conceived that the ligand's potential to behave as an electron reservoir may trigger radical chemistry at its backbone.[6]

To design an efficient base metal assisted catalyst, herein we have introduced an odd alternant hydrocarbon, phenalenyl (PLY) based ligand. PLY is a well-known building block for constructing organic radical based materials for its ability to exist in three redox active states such as cation, neutral radical and anion by accepting corresponding electrons into its nonbonding molecular orbital (NBMO).[7] In this work, we take advantage of the NBMO in metal coordinated PLY based ligand which readily stabilizes the radical state[8] making it a unique redox non-innocent ligand. We have recently established that a metal coordination of phenalenyl ligand is essential for ready acceptance of electrons in the PLY ligand backbone.[9] By this way, we have constructed a zinc-PLY based spin memory device[9a] and designed PLY based iron(III) complex displaying an excellent electrocatalytic property as cathode material for one compartment membraneless H_2O_2 fuel cell.[9b] Very recently, the development of metal coordinated PLY radical and their use in diverse areas spanning from catalysis to spin-electronics has been reviewed.[10] In this work, we hypothesize that injected electrons via chemical reduction into the metal coordinated PLY system can be stored and utilized during the catalytic process, which can avoid attaining unfavorable oxidation state of the metal center. This report further discloses that the redox participation of the PLY ligand with coordinated Ni(II) results an excellent catalyst to perform regioselective anti-Markovnikov hydrosylilation[11] of a wide variety of olefins. It might be worth noting that the base metal catalyzed hydrosilylation of alkenes is of great interest and has been pioneered by Chirik and coworkers.[3b]

[a] *Department of Chemical Sciences, Indian Institute of Science Education and Research-Kolkata ,Mohanpur-741246, India.*
E-mail: swadhin.mandal@iiserkol.ac.in
[b] *Department of Chemical Sciences, Indian Institute of Science Education and Research Mohali, SAS Nagar 140306, India*
E-mail: adhikari@iisermohali.ac.in

Electronic Supplementary Information (ESI) available: Detailed experimental procedures, spectra (NMR, and HRMS), CV, crystallographic details, and coordinates of the computed structures. See DOI: 10.1039/x0xx00000x

View Article Online
DOI: 10.1039/C7SC04687A

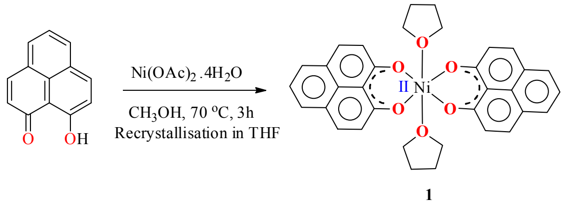

Scheme 1 Synthesis of catalyst **1**.

Results and Discussion

The PLY-nickel(II) complex, **1** (Scheme 1) was prepared by treating $Ni(OAc)_2.4H_2O$ with two equivalents of the ligand, 9-hydroxyphenalenone in methanol at 60 °C to give a crystalline precipitate. Analytically pure **1** was obtained by recrystallization of the dried reaction mixture in dry THF at 5 °C yielding dark orange colored crystals of **1** in nearly 90% yield. Complex **1** was paramagnetic and characterized by an array of analytical tools including elemental analysis, ESI-MS, IR, and single crystal X-ray diffraction studies. The molecular structure of **1** was revealed by single crystal X-ray diffraction and it shows a tetragonal ligand environment for a six coordinate nickel(II) ion. The ORTEP diagram (Fig. 1) displays that Ni^{II} ion is coordinated to four O-donor atoms of two phenalenone ligands (O1 and O2 atoms as coordination site) and the axial positions are occupied by two THF ligands. The solid state magnetic susceptibility of **1** was measured revealing a magnetic moment of 2.82 μ_B, fully corroborating with the octahedral Ni^{II} picture (Fig. 2, see later).

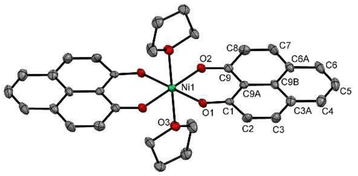

Fig. 1 Perspective ORTEP view of the molecular structure (50% ellipsoid level) of **1**, where hydrogen atoms are omitted for the sake of clarity.

Anticipating that PLY may act as a redox storage motif, electrochemical reduction of **1** was performed by cyclic voltammetry, which evinced two quasi-reversible one-electron waves at −1.26 and −1.52 V (vs SCE, Fig. S1, ESI). This is indicative of sequential one-electron reductions at the PLY ligand backbone, as inferred previously from the study on a similar $Fe(PLY)_3$ system.[9b] This reduction process generates a PLY-based radical and bi-radical species, respectively (Scheme 2) which was also observed in a series of spiro-bis-phenalenyl compounds, reported previously.[12] Also the difference between the first reduction potential $E^1_{1/2}$ and 2nd reduction potential $E^2_{1/2}$ ($\Delta E^{2\text{-}1}$ = 0.26 V) matches very well with earlier electrochemical results.[8a] It may be noted that $\Delta E^{2\text{-}1}$ is considered as the disproportionation potential which is directly correlated with the on-site Coulomb correlation energy (U).[8a] The $\Delta E^{2\text{-}1}$ value is also in close agreement to bis-phenalenyl-boron complexes bearing the same O,O-phenalenyl ligand ($\Delta E^{2\text{-}1}$ values are -0.29 V and -0.28 V), strongly suggesting clear successive two step one-electron reductions into phenalenyl moiety.[8a] After having this clue, two electrons were chemically injected to **1** by reduction with potassium yielding a green paramagnetic complex **2** (*vide infra* on its magnetism and electronic structure). This observation encouraged us to check if such two-electron reduced species **2** can initiate any single electron transfer (SET) process to activate Si-H bond of the silane. Notably, we have used reduced phenalenyl radical for SET process in designing transition metal free catalysis for C-H functionalization very recently.[13] Accordingly, an equimolar mixture of Ph_2SiH_2 and 1-octene was examined in the presence of 0.25 mol% of complex **1** and three equiv. of potassium in THF solution under anaerobic atmosphere. To our great delight, a quantitative conversion to the anti-Markovnikov hydrosilylated product[14] was observed after 30 minutes at rt (Table 1, entry 2). The hydrosilylation under our chosen condition is very clean and devoid of any other by-product formation resulting from isomerization, dimerization or hydrogenation of olefins.[11,14] Gratifyingly, we also observed nearly complete conversion when $PhSiH_3$ and Ph_3SiH were used as silanes (Table 1, entries 1 and 3). However, scanning the reaction with other silanes such as Ph_2MeSiH, $(EtO)_3SiH$, $(MeO)_3SiH$ or Et_3SiH led to much lower yield (up to 45%, Table 1, entries 4-7). The control experiments using Ph_2SiH_2 as the representative silane clearly established that without catalyst the reaction did not proceed when other conditions were kept identical (Table 1, entry 8). Furthermore, addition of potassium (sodium also works as a reductant but yields 70% product) is necessary for this catalytic reaction to proceed (Table 1, entry 9). However, an organic amine tetrakis(dimethylamino)ethylene (TDAE), which is a much milder reducing agent than K or Na was unable to deliver any product (Table 1, entry 10). It was finally concluded that both catalyst **1** and a suitable reducing agent are necessary for this catalysis (Table 1, entry 11) since the PLY-based biradical is generated *in situ*. Several earlier reports on nickel catalyzed hydrosilylation also involve *in situ* generation of the catalytically active species by various external reductants such as $LiAlH_4$, EtMgBr, $NaBEt_3H$ etc.[15] A recent report also discloses that the nickel catalyzed silane activation and hydrosilylation can be performed across a Ni–Ni bond, utilizing the redox non-innocence of the naphthyridine-diimine ligand.[16]

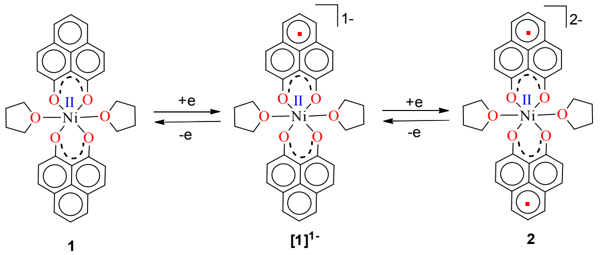

Scheme 2 Two successive one electron reductions showing the formation of phenalenyl-centered anionic radical and di-anionic species, respectively

Furthermore, to establish that the PLY-based nickel complex is essential for the reaction, we performed catalysis with only $NiCl_2$ as well as $NiCl_2$/K combination which did not result any hydrosilylated product (Table 1, entries 12-13) under identical conditions adopted for catalyst **1**. To substantiate the crucial role of the PLY ligand as a redox reservoir during the catalysis, we further conducted another control experiment with $Ni(acac)_2$ or $Ni(acac)_2(MeOH)_2$ (acac = acetylacetonate) complex,[17] assuming that the coordination environment of Ni in these complexes closely mimics the coordination environment of catalyst **1.** The hydrosilylation performed with $Ni(acac)_2$/K or $Ni(acac)_2(MeOH)_2$/K combination resulted in extremely small amount of product (below 5%, Table 1,

View Article Online
DOI: 10.1039/C7SC04687A

entries 14 and 15) under identical conditions (opposed to 99% for **1**/K combination, Table 1, entry 2). This result provides significant support to the hypothesis that redox active PLY based ligand plays an important role as electron reservoir, which facilitates redox chemistry upon reduction with K metal. Moreover, the efficacy of our catalyst is impressive, since it can even operate at a miniscule loading (0.05 mol%, Table 1, entry 16) translating to a turnover number of 1200. With this initial result in hand, we investigated the substrate scope further for the functionalized olefins using Ph_2SiH_2 as the silane source. As summarized in Chart 1, 1-hexene, 5-bromo-1-pentene and 4-bromo-1-butene show essentially complete conversion to the corresponding organosilanes (**3a**, **3b** and **3c**, respectively) within 30 min. at rt. The formation of anti-Markovnikov product was noticed exclusively in all cases. Interestingly, hydrosilylation of an unstrained internal olefin, 2-octene, also took place smoothly to deliver only the terminally silylated product (**3d**) in 97% yield, most likely via successive olefin isomerization and hydrosilylation. Moreover, hydrosilylation of 1,5-hexadiene successfully resulted in the disilylated product 1,6-bis(diphenylsilyl)hexane (**3e**) with 2 equiv. of Ph_2SiH_2. This is a clear improvement, since hydrosilylation of dialkenes such as 1,5-hexadiene has earlier been very problematic.[18] The versatility of the substrate scope was further evidenced by successful silylation of vinyl cyclohexyl ether, vinyl butyl ether and phenyl allyl ether which were quantitatively converted to the corresponding anti-Markovnikov products (**3f**, **3g** and **3j**, respectively) within an hour. Excellent functional group tolerance was also achieved with anti-Markovnikov selectivity as tested with a group of various aromatic substrates. The allylbenzene and 4-methoxy allylbenzene can be completely converted to the corresponding linear products (**3h** and **3i**) within an hour. Further experiments exhibited that presence of esters and tertiary amines are well tolerated providing expected chemoselective hydrosilylated products (**3k-3n**) in excellent isolated yield.

Table 1 Standardization of catalytic activity with different silanes for the hydrosilylation of 1-octene.[a]

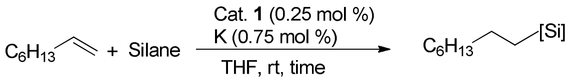

Entry	Catalyst	Silane	Time (h)	Yield (%)[b]
1	**1**	$PhSiH_3$	1	99
2	**1**	Ph_2SiH_2	0.5	99
3	**1**	Ph_3SiH	1	95
4	**1**	Ph_2MeSiH	3	45
5	**1**	$(EtO)_3SiH$	3	55
6	**1**	$(MeO)_3SiH$	3	20
7	**1**	Et_3SiH	10	<5
8[c]	-	Ph_2SiH_2	10	-
9[d]	**1**	Ph_2SiH_2	10	-
10[e]	**1**	Ph_2SiH_2	0.5	-
11[f]	-	Ph_2SiH_2	10	-
12[d]	$NiCl_2$	Ph_2SiH_2	0.5	-
13	$NiCl_2$	Ph_2SiH_2	0.5	-
14	$Ni(acac)_2$	Ph_2SiH_2	0.5	<5
15	$Ni(acac)_2(MeOH)_2$	Ph_2SiH_2	0.5	<5
16[g]	**1**	Ph_2SiH_2	0.5	60

[a] Typical conditions: Catalyst **1** (0.25 mol %), K (0.75 mol%), alkene (1.00 mmol), 1 equiv. silane, THF (1 mL), RT. [b] The reported yields are ^1H NMR spectroscopic yields. [c] No catalyst **1**. [d] No K. [e]Reaction with TDAE. [f] In absence of catalyst **1** and K. [g] Catalyst **1** with 0.05 mol %.

Chart 1 Nickel-catalyzed hydrosilylation of terminal alkenes.[a]

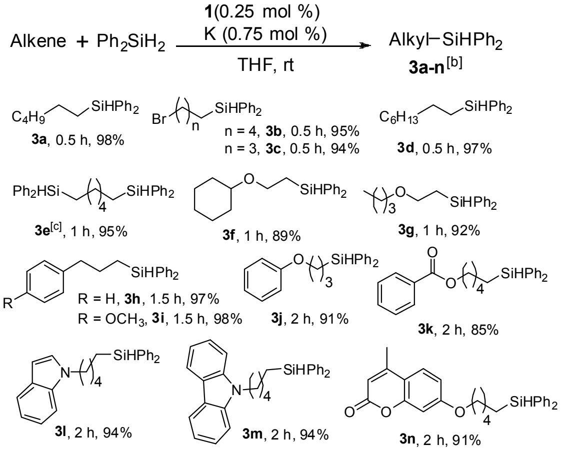

[a] Reaction conditions: alkene (0.5 mmol), Ph_2SiH_2 (1 equiv.), **1** (0.25 mol%), K (0.75 mol%) THF (1 mL), rt. [b] Yields are reported after purification by column chromatography. [c] 2 equiv of Ph_2SiH_2 added.

Table 2 Double alkylation reaction of alkenes with $RSiH_3$ (R = Ph, Bu).[a]

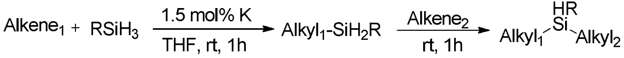

Entry	$Alkene_1$	R	$Alkene_2$	Product	Yield (%)[b]
1	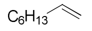	Ph	–	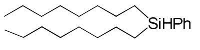	96
2	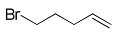	Ph	–	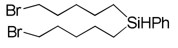	95
3[c]	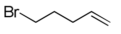	Bu	–	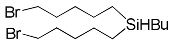	97
4[c]	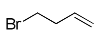	Bu	–	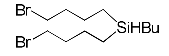	97
5	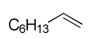	Ph	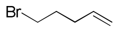	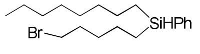	89
6	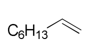	Ph	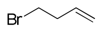	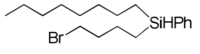	92
7[c]	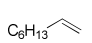	Bu	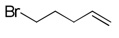	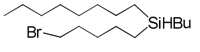	93
8[c]	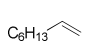	Bu	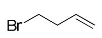	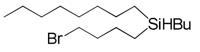	91
9	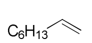	Ph	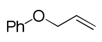	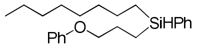	85
10	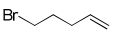	Ph	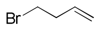	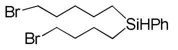	92

[a] Reaction conditions: **1** (0.5 mol%), K (1.5 mol%), $alkene_1$ (0.5 mmol), $RSiH_3$ (1 equiv.), $alkene_2$ (0.5 mmol), THF (1 mL), rt. [b] Isolated yields after purification by column chromatography. [c] *t* = 6h

Inspired by these results, we became interested in further exploring the scope of this methodology for the double hydrosilylation method. Usually, the double alkylation of silane to produce dialkylated product by adding one more equivalent of alkene in the same reaction mixture is potentially problematic.[19] In our case, hydrosilylation of 2:1 molar ratio of alkene with $RSiH_3$ (R =

View Article Online
DOI: 10.1039/C7SC04687A

Ph, Bu) yielded the corresponding dialkyl silylated product R(alkyl)$_2$SiH exclusively (Table 2, entries 1-4). However, the dialkylated silane product remained inactive toward further hydrosilylation. We have also studied the double alkylation of hydrosilane with one equiv. RSiH$_3$ and step wise addition of two different alkenes (Table 2, entries 5- 10). For example, (5-bromopentyl)(octyl)(phenyl)silane was obtained in 89% yield by addition of 1-octene and 5-bromopentene sequentially (Table 2, entry 5) in a single pot. We believe that such smooth silylation reactions under very mild conditions likely results from the redox tuning between PLY and Ni^{II} orbitals.

In the context of synthesizing silicones, the alkylation of polymethylhydrosiloxane (PMHS) is one of the most common chemical methods. A large variety of catalysts mostly comprising of expensive platinum has been studied for the modification of siloxanes.[20] To the best of our knowledge, there is no efficient nickel based catalyst for hydrosilylation of alkenes with PMHS as a precursor silane. This fact prompted us to examine the competency of **1** towards hydrosilylation by PMHS. Model hydrosilylation of different alkenes (1-octene and 1-hexene) using heptamethyltrisiloxane yielded anti-Markovnikov addition products hexyl-1,1,1,3,5,5,5- and octyl-1,1,1,3,5,5,5 heptamethyltrisiloxane (**4a** and **4b**, respectively) in 79% and 84% isolated yields (Scheme 3). It may be noted that the product **4a** is a commercially available agricultural adjuvant as well as a sensory and performance enhancer in cosmetic formulations.[11b] Next, we carried out the hydrosilylation of 1-octene and 1-hexene with PMHS containing approximately 50 Si-H units resulting in corresponding hydrosilylated products (**4c** and **4d).** These are important intermediates towards the functionalization of silicones[14,20] and obtained in nearly quantitative yield.

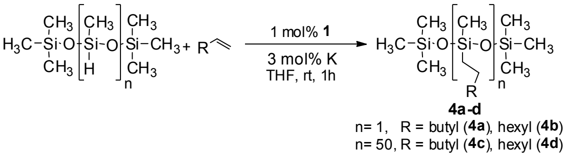

Scheme 3 The hydrosilylation of olefins by siloxanes.

To understand the mechanistic pathway for this fascinating reaction, first we have conducted the catalysis by adding 1 eqv. K with respect to **1**, which revealed that the reaction does not proceed at all. Then we checked whether **2** (two electron reduced product of **1**, see drawing in Scheme 2) can act as an active catalyst for the hydrosilylation reaction. We isolated the radical **2** as a green solid in bulk by performing the reduction of **1** with K metal using dry THF strictly under dry nitrogen atmosphere. After isolation, **2** was dried and stored in a nitrogen filled glovebox. The reaction of 1-octene or allylbenzene with Ph$_2$SiH$_2$ in the presence of a catalytic amount of complex **2** (0.25 mol%) in THF afforded corresponding anti-Markovnikov products in 98% and 95% yields, almost identical to the yields via *in situ* catalytic protocol (99%, Table 1, entry 2 and 97%, Chart 1, **3h**). The bulk isolation and storage of compound **2** ensures that the catalysis can be accomplished without involving K metal in every catalytic run.

The direct role of **2** in hydrosilylation catalysis prompted us to investigate the electronic structure of **2** in the light of redox noninnocence of the PLY backbone. Since our electrochemical experiments revealed that the reductions of **1** are predominantly ligand based (*Vide supra* and references therein),[9,10] three spin states may be envisaged for **2** (Scheme 4). Upon two electron reduction to **1**, either it may generate a fully AF-coupled singlet (diamagnetic), or an AF-coupled triplet or a quintet state (Scheme 4). Among these choices, the first one is easily discarded since **2** is paramagnetic (magnetic data in Fig. 2). To interrogate this spin ground state of **2** between second and third choices, we conducted solid state magnetometry measurement by SQUID varying the temperature from 300 to 2K (Fig. 2). This analysis discloses that the magnetic moment of **2** is 3.42 μ_B at RT and decreases smoothly to reach a value 1.52 μ_B at 20 K. This sharp drop of magnetic moment with lowering of temperature is a clear signature of AF-coupling.[21] The μ_{eff} at RT is smaller than that expected for S=2 system, however it is very close to 3.44 μ_B, a spin-only value anticipated for ground state comprising of isoenergetic S=1 and S=2 states. To arrive at this value, the general formula $\mu_{total}=[(\mu_A)^2+(\mu_B)^2]^{1/2}$ is used when two isolated spin ground states A and B are degenerate.[22] In our case, the calculated magnetic moment becomes $[3/8*(2.83)^2 + 5/8*(3.74)^2]^{1/2} = 3.44\ \mu_B$, considering the spin only values for the states (S=1 and S=2) and factoring their respective degeneracies. The experimentally

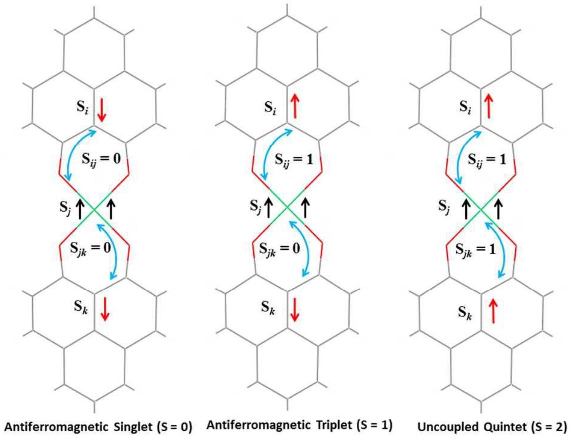

Scheme 4 Schematic representation of possible electronic spin states of compound **2** where two ligand based electrons are interacting with high spin Ni$^{(II)}$.

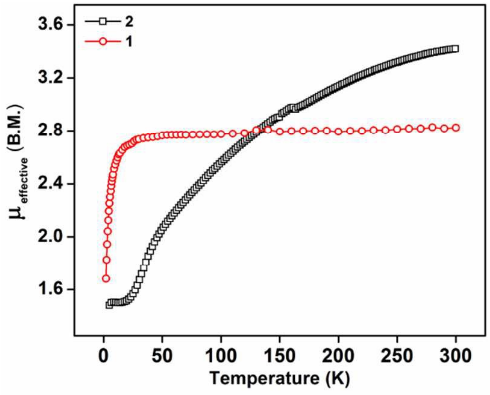

Fig. 2 Variation of μ_{eff} values as a function of temperature for compound **1:** 2.82 μ_B at 300 K (before reduction, in red) and **2:** 3.42 μ_B at 300 K (after reduction, in black) revealing the presence of two unpaired spins in compound **1** and four unpaired spins in compound **2** at rt.

View Article Online
DOI: 10.1039/C7SC04687A

observed value is very close to the theoretically projected value, which strongly supports the near degeneracy of the two spin states. Furthermore, as will be reported below, DFT calculations suggest that the AF-coupled triplet and the quintet states are indeed iso-energetic. Our conclusion from the SQUID experiment is that the **2** possesses an AF-coupled triplet (*vide infra*) as the ground state, although a quintet state is highly accessible over a wide range of temperature. The paramagnetic **2** is EPR silent (X-band) at both room and low temperature which is hardly surprising for a non-Kramers $S=1$ spin system.[23] To find a concrete spectroscopic signature for the proposed AF-coupled triplet ground state of **2**, we attempted to find the spin forbidden ($\Delta S=\pm2$) transition at the half-field strength of the applied magnetic field, by performing parallel mode EPR spectroscopy in dry DMSO at 5K. Unfortunately, the signature of such half-field signal was not observed, which may be attributed to the high zero field splitting associated with Ni(II) ion.[24] Both CV and SQUID magnetometry data clearly preclude the possibility of the metal-centered reduction leading to diamagnetic Ni^0 (*vide infra* for electronic structure of **2**). We scrutinized this fact further by recording X-ray photoelectron spectroscopy (XPS) of both **1** and **2** (Fig. S2, ESI). The XPS data displays that for **2**, the 2P$_{3/2}$ transition occurs at 854.7 eV along with characteristic satellite peak at 860.2 eV. This peak corresponds to Ni(II) and remains same in both **1** and **2**.[25] The identical peak position for complexes before and after reduction supports that the oxidation state for nickel is completely retained upon reduction.

To further shed light on the electronic structure details of **2** we resorted on high-level DFT calculations. The analysis of molecular orbitals exposes that the LUMO for both **1** (Fig. S3a, ESI) and its one-electron reduced product (Fig. S3b, ESI) are completely ligand localized. This fact strongly suggests that the PLY ligand can accept and hold electron (Fig. S5, ESI for spin density in single-electron reduced product) so that the oxidation state for nickel remains constant to Ni^{II} during the reduction processes. Indeed, at the B3LYP/6-31+G* (lanl2dz pseudopotential for Ni) level of calculations, we probed that the two-electron reduced product, **2** to possess an antiferromagnetically (AF) coupled triplet as the ground state with a very low-lying excited quintet state. The $\langle S^2 \rangle$ value obtained for the AF-coupled triplet electronic structure was 2.11, which reflects slight amount of spin contamination and thus lends credence to the ground state energy value. As we have discussed earlier, this electronic structure is fully consistent with the SQUID results. The broken symmetry solution[26] for AF-coupled triplet is clearly depicted by the spin density plot of **2** (Fig. 3). This proves that the electrons donated during reductions are housed by two PLY frameworks. One of the ligand-based electrons is likely AF-coupled with nickel-centric electron which results in two unpaired electrons distributed over the nickel and other PLY ligand, overall amenable to a triplet ground state. This proposition does not preclude other weak exchange coupling schemes to arrive at the AF-coupled singlet state though. Additionally, the electron donation to the ligand-centric low lying LUMO can easily be traced by the respective C−C bond length changes of the reduced ligand backbone (Fig. S4, ESI). Moreover, the natural population analysis performed on the symmetry broken densities of **2** exposes that the 3d orbital population is 8.2, which further proves the presence of Ni$^{(II)}$.[27]

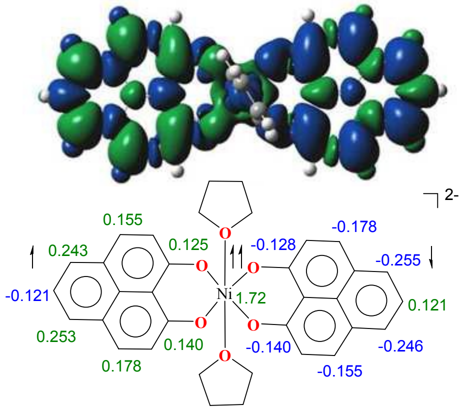

Fig. 3 The spin density plot for **2**, where colour coding refers to green, excess α and blue, excess β spin. The contour values was set to ± 0.0004 (**e.**bohr^{-3})$^{1/2}$(above). The major numerical values of excess spin densities are shown (below).

Given this electronic picture of **2** in mind, we anticipated that the olefin hydrosilylation may follow a radical pathway. To check this assertion further, a radical scavenger TEMPO was added (two runs with 1 and 2 equiv.) to the reaction mixture which drastically reduced the yield of the hydrosilylated product to 43% and 15%, respectively (see Scheme S1, ESI). The same radical quenching was also performed by galvinoxyl radical (used two equiv.) which fully restricted the reaction (see Scheme S2, ESI). Based on these preliminary findings, a plausible reaction mechanism has been proposed involving a radical pathway (Scheme 5). A single electron transfer (SET) occurs from **2** to silane to generate a silyl radical which subsequently adds to the olefin resulting in the formation of a silylated alkyl radical (**I**). The generation of silyl radical during this hydrosilylation has been unambiguously authenticated by trapping the TEMPO-adduct of the putative radical, **6**. The radical mechanism is also in accord with our recent report, where K-complex of PLY can participate in catalytic SET process to accomplish transition metal free C–C coupling catalysis.[13] Upon SET, **2** transforms into an anionic monoradical species comprising nickel hydride, **5**. The silylated alkyl radical **I** subsequently reacts with a hydrogen atom originated from the nickel hydride species **5**. This hydrogen atom transfer (HAT) from the metal hydride to result in the silylated alkane closely resembles many transition metal hydride promoted hydrogenation of olefins where a radical is involved. Some classic studies by Halpern and Norton have shown that hydrogenation of anthracene and styrenes via HMn(CO)$_5$ generates a carbon based radical via HAT.[28] Encouragingly, the intermediacy of **I** has also been proved by trapping TEMPO-adduct, **7** by mass spectrometry. The anti-Markovnikov selectivity in our hydrosilylation reaction is fully anticipated since the silyl radical addition to the olefin will only engender a stable secondary carbon radical in contrast to a primary one. During the HAT to **I** furnishing the final product, one electron comes back to the catalyst and housed in the ligand backbone, thus regenerating **2**. Notably, this type of silyl radical mediated hydrosilylation of alkene has been proposed in several earlier reports.[29] Moreover, ligand-based redox promoting homolytic cleavage of X-H bond has recently been reported, which provides further support to our mechanistic postulate.[30] Our proposed

View Article Online
DOI: 10.1039/C7SC04687A

mechanistic hypothesis is clearly different from conventional Chalk-Harrod[31] or modified Chalk-Harrod mechanism[32] of hydrosilylation which is often operative in precious metal based catalysis. It also differs from Chirik's recent report, where oxidative addition of $(EtO)_3Si–H$ happens at the nickel center which is supported by a redox non-innocent aryl-substituted α-diimine ligand.[33]

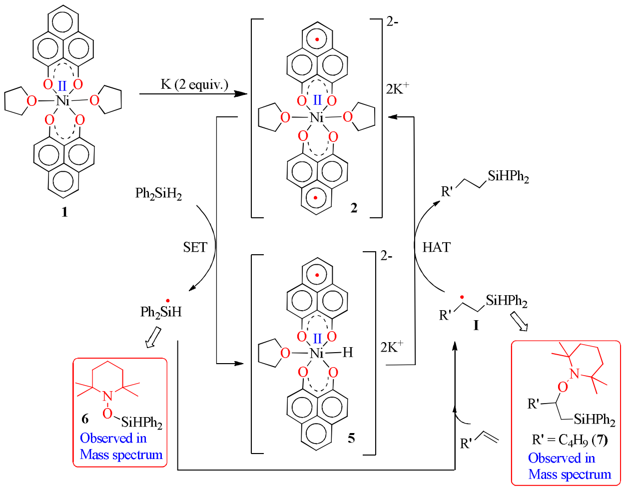

Scheme 5 A plausible mechanism for catalytic hydrosilylation of olefin by **1** through PLY based radical initiation.

Conclusions

In summary, using the storage property of the redox equivalent for a PLY ligand, we have been able to synthesize a very efficacious nickel assisted catalytic system to carry out olefin hydrosilylation under mild condition. The ligand centered radicals upon reduction of **1** made this catalysis feasible. It may be noted that although PLY centered radical is well-known for over five decades, their use in electron transfer catalysis is an evolving area and this study establishes that there is an enormous future promise to design base metal-assisted PLY based radical to develop catalysts for multifarious organic transformations. Our current focus resides on developing more base metal catalysts using ligand based electrons and understanding the fascinating electronic structure of the exchange-coupled systems which are responsible to deliver catalysis.

Experimental Section

General considerations.

All manipulations were performed under a dry and oxygen free atmosphere (argon) using standard Schlenk techniques or inside a glovebox maintained below a 0.1 ppm of O_2 and H_2O. All glassware were oven-dried (130 °C) and evacuated while hot prior to use. All solvents were distilled from Na/benzophenone prior to use. All other chemicals were purchased from Sigma–Aldrich and used as received. The HRMS data were obtained using a Finnigan MAT 8230 instrument. The ESI-MS data were obtained using the maXis impact™ mass spectrometer. Elemental analyses were carried out using a PerkinElmer 2400 CHN analyzer, and samples were prepared by keeping them under reduced pressure (10^{-2} mbar) overnight. The melting points were measured in a sealed glass tube on a Büchi B-540 melting point apparatus. Analytical TLC was performed on a Merck 60 F254 silica gel plate (0.25 mm thickness). ^{1}H, ^{13}C and ^{29}Si NMR spectra were recorded on a JEOL ECS400 MHz spectrometer and on a Bruker AvanceIII 500 MHz spectrometer. EPR was recorded on a JEOL JES-FA200 X-band spectrometer. All chemical shifts were reported in ppm using tetramethylsilane as a reference. Electrochemical analyses were performed by using a three-electrode system on a Princeton Applied Research 263A electrochemical workstation. CV was recorded in THF using Pt working electrode, Pt-wire as the counter electrode and SCE as the reference electrode. $TBAPF_6$ (0.1 M in dry THF) was utilized as the supporting electrolyte. Electrochemical analysis was executed in an inert atmosphere. Electrochemical analysis was executed in an inert atmosphere. Phenalenyl (PLY) ligand was prepared according to the literature procedure.[34]

Procedure for the synthesis of 1.

In a 100 mL round bottom flask, PLY (0.98 g, 5mmol) was dissolved in 60 mL MeOH upon heating at 60 ^{o}C. Separately, a 100 mL conical flask was taken and $Ni(OAc)_2.4H_2O$ (0.62 g, 2.5 mmol) was dissolved in 30 mL MeOH. To the hot methanolic solution of PLY ligand, the solution of $Ni(OAc)_2$ dissolved in methanol was added dropwise. The yellow solution was turned darker and slowly bright orange precipitate started forming. The reaction mixture was stirred vigorously with heating at 60 ^{o}C for another 3 h and then the reaction mixture was allowed to cool at rt. Subsequently the precipitate was filtered. The precipitate was washed repeatedly with MeOH to remove any unreacted ligand and metal salt. The title compound was recrystallized from THF. Crystals suitable for SCXRD were grown by dissolving the recrystallized material in dry THF and keeping at 4 ^{o}C in a Schlenk flask for 1-2 weeks. Yield 90%. Uv-visible (THF) λ max/nm (ε in $M{-}1cm^{-1}$): 288(10931), 351(38000), 413(9220), 436 (17542), 463(16867). FT-IR(thin film) ν(cm^{-1}): 3695.15, 2693.20, 1627.97, 1518.88, 1433.84, 1345.45, 1260.30, 1095.77, 901.58, 749.65. ESI-MS: m/z calc. for $C_{34}H_{31}NiO_6$ $[M+H]^+$ 593.1474, found 593.1468. Elemental analysis: Anal. Calcd for $C_{34}H_{30}NiO_6$: C, 68.83; H, 5.10. Found: C, 68.88; H, 5.17.

General procedure for the hydrosilylation of functionalized alkenes with catalyst 1.

To a stirred solution of **1** (1.5 mg. 0.0024 mmol) and K (0.30 mg, 0.0074 mmol) in THF (1 mL), the silane (1 mmol) and alkene (1.00 mmol) were added at room temperature. The solution was stirred at room temperature, and the progress of the reaction was monitored by ^{1}H NMR spectroscopy. After completion of the reaction, hexamethyl benzene (120 mg, 1.00 mmol) was added as an internal standard to the reaction mixture. The ^{1}H NMR analysis of the resulting solution revealed the formation of product. The solution was concentrated under vacuum, and the residue was purified by column chromatography using hexane as an eluent. The final product was characterized by ^{1}H, ^{13}C and ^{29}Si NMR spectroscopy.

General procedures for double alkylation of alkenes with $PhSiH_3$.

To a stirred solution of **1** (1.5 mg, 0.0024 mmol) and K (0.3 mg, 0.0075 mmol) in THF (1 mL), silane (0.5 mmol) and alkene (0.5 mmol) were added at room temperature and the solution was stirred at room temperature. After 1 h, another 0.5 mmol of alkene was added to the reaction mixture and stirred at room temperature for 1 h. The progress of the reaction was monitored by ^{1}H NMR spectroscopy. After completion of the reaction, hexamethyl benzene (60 mg, 0.50 mmol) was added as an internal standard to

View Article Online
DOI: 10.1039/C7SC04687A

the reaction mixture. The ^{1}H NMR spectroscopic analysis of the resulting solution revealed the formation of product. The solution was concentrated under vacuum, and the residue was purified by column chromatography using hexane as an eluent. The final product was characterized by ^{1}H, ^{13}C and ^{29}Si NMR spectroscopy.

Procedure for the hydrosilylation of alkenes with 1,1,1,3,5,5,5-heptamethyltrisiloxane (HMTS).

To a stirred solution of **1** (2.96 mg, 0.0049 mmol) and K (0.6 mg, 0.015 mmol) in THF (1 mL), siloxane (0.5 mmol) and alkene (0.5 mmol) were added at room temperature. The solution was stirred at room temperature. The progress of the reaction was monitored by ^{1}H NMR spectroscopy. After completion of the reaction, hexamethyl benzene (0.50 mmol) was added as an internal standard to the reaction mixture. The ^{1}H NMR spectroscopic analysis of the resulting solution revealed the formation of product. The solution was concentrated under vacuum, and the residue was purified by column chromatography using hexane as an eluent. The final product was characterized by ^{1}H, ^{13}C and ^{29}Si NMR spectroscopy.

Procedure for the hydrosilylation of alkenes with polymethyl hydrosiloxane (PMHS).

To a stirred solution of **1** (2.96 mg, 0.0049 mmol) and K (0.6 mg, 0.015 mmol) in THF (1 mL), siloxane (0.5 mmol) and alkene (50 equv.) were added at room temperature. The solution was stirred at room temperature. The progress of the reaction was monitored by ^{1}H NMR spectroscopy. After completion of the reaction, hexamethyl benzene (0.50 mmol) was added as an internal standard to the reaction mixture. The ^{1}H NMR spectroscopic analysis of the resulting solution revealed the formation of product. The solution was concentrated under vacuum, and the residue was purified by column chromatography using hexane as an eluent. The final product was characterized by ^{1}H and ^{13}C NMR spectroscopy.

Procedure for the preparation of compound 2.

1 and potassium were taken in 1:3 ratio using dry THF as a solvent. The resulting mixture was allowed to stir for 10 min at room temperature, when a green precipitate was formed. The solvent was evaporated under high vacuum when **2** was obtained as a green solid. The spin state of **2** was characterized by SQUID and X-ray photoelectron spectroscopy and further electronic structure was calculated by DFT. All our attempts to collect elemental analysis data or mass spectroscopic data of the radical **2** did not succeed which may be attributed to its high sensitivity in air and moisture.

Computational Details.

All calculations were carried out using Density Functional Theory as implemented in the Gaussian 09[35] quantum chemistry programs. The geometries of stationary points were optimized with the generalized gradient approximation (GGA) by means of the Becke exchange functional along with Lee, Yang, Parr correlation functional (LYP). We used double-ζ basis set with the relativistic effective core potential of Hay and Wadt (LANL2DZ) for the nickel atom and 6-31+G(d) basis set for other elements (H, C, O). The geometries were optimized without any symmetry constraints. For the optimization, full model was chosen with furan as the weakly coordinating ligand. The symmetry broken DFT solution was detected using the Gaussian keyword Stable=opt. Harmonic force constants were computed at the optimized geometries to characterize the stationary points as minima. The molecular orbitals were visualized and spin density was plotted using Gaussview.

X-ray crystallographic details.

Single crystal of compound **1** was mounted on a glass pip. Intensity data were collected on a SuperNova, Dual, Mo at zero, Eos diffractometer. The crystals were kept at 100 K during data collection. Atomic coordinates, isotropic and anisotropic displacement parameters of all the nonhydrogen atoms of two compounds were refined using Olex2,[36] and the structure was solved with the Superflip[37] structure solution program using Charge Flipping and refined with the ShelXL[38] refinement package using Least Squares minimization.

SQUID details.

SQUID magnetometer (Quantum Design MPMS) was used to investigate the magnetic properties (Magnetic susceptibility) of the compounds. We have used a light weight homogeneous quartz tube as a sample holder for the magnetic measurements in SQUID MPMS-XL5 to minimize the background noise and stray field effects. The magnetic data were corrected for the diamagnetic contribution from the sample holder by measuring the magnetic moment of the sample holder with an air gap corresponding to the sample length. The intrinsic diamagnetism of the samples was corrected by the standard literature using Pascal's constants.

Conflicts of interest

There is no conflict to declare.

Acknowledgements

We thank SERB (DST), India (Grant No. SR/S1/IC-25/2012) for financial support. GVK thanks UGC for a research fellowship. AP thanks SERB for a fellowship. BKS acknowledges support from SERB for a NPDF fellowship (PDF/2016/000213). DA thanks his mentors, Prof. Daniel J. Mindiola (Upenn) and Sonbinh T. Nguyen (Northwestern) for training and encouragement. We thank Dr.s Vishal Rai and Sanjit Konar (IISER Bhopal) for their help in recording HRMS and SQUID data. We thank Dr. Parthasarathi Bera (NAL, Bangalore) for XPS measurement. We are thankful to Prof. Olav Schiemann (University of Bonn, Germany) for his help in parallel mode EPR measurements on compound **2**.

References

1 (a) V. Lyaskovskyy and B. de Bruin, *ACS Cat.*, 2012, **2**, 270-279; (b) P. J. Chirik and K. Wieghardt, *Science*, 2010, **327**, 794-795.

2 (a) K. Hindson and B. de Bruin, *Eu. J. Inorg. Chem.*, 2012, **2012**, 340-342; (b) W. I. Dzik, J. I. van der Vlugt, J. N. H. Reek and B. de Bruin, *Angew. Chem., Int. Ed.*, 2011, **50**, 3356-3358; (c) W. Kaim, *Eu. J. Inorg. Chem.*, 2012, **2012**, 343-348.

3 (a) M. W. Bouwkamp, A. C. Bowman, E. Lobkovsky and P. J. Chirik, *J. Am. Chem. Soc.*, 2006, **128**, 13340-13341; (b) A. M. Tondreau, C. C. H. Atienza, K. J. Weller, S. A. Nye, K. M. Lewis, J. G. P. Delis and P. J. Chirik, *Science*, 2012, **335**, 567-570.

4 (a) K. J. Blackmore, J. W. Zille and A. F. Heyduk, *Inorg. Chem.*, 2005, **44**, 5559-5561; (b) C. Stanciu, M. E. Jones, P. E. Fanwick and M. M. Abu-Omar, *J. Am. Chem. Soc.*, 2007, **129**, 12400-12401.

5 A. L. Smith, K. I. Hardcastle and J. D. Soper, *J. Am. Chem. Soc.*, 2010, **132**, 14358-14360.

6 A. T. Radosevich, J. G. Melnick, S. A. Stoian, D. Bacciu, C.-H. Chen, B. M. Foxman, O. V. Ozerov and D. G. Nocera, *Inorg. Chem.*, 2009, **48**, 9214-9221.

View Article Online
DOI: 10.1039/C7SC04687A

7 (a) R. C. Haddon, *Nature*, 1975, **256**, 394-396; (b) M. E. Itkis,; X. Chi, A. W. Cordes and R. C. Haddon, *Science*, 2002, **296**, 1443-1445; (c) R. G. Hicks, *Nat. Chem.*, 2011, **3**, 189-191; (d) Y. Morita, S. Suzuki, K. Sato and T. Takui, *Nat. Chem.*, 2011, **3**, 197-204.

8 (a) S. K. Mandal, S. Samanta, M. E. Itkis, D. W. Jensen, R. W. Reed, R. T. Oakley, F. S. Tham, B. Donnadieu and R. C. Haddon, *J. Am. Chem. Soc.*, 2006, **128**, 1982-1994; (b) B. Marciniec, *Coord. Chem. Rev.*, 2005, **249**, 2374-2390; (c) T. K. Sen, A. Mukherjee, A. Modak, P. K. Ghorai, D. Kratzert, M. Granitzka, D. Stalke and S. K. Mandal, *Chem.– Eur. J.*, 2012, **18**, 54-58; (d) T. K. Sen, A. Mukherjee, A. Modak, S. K. Mandal and D. Koley, *Dalton Trans.*, 2013, **42**, 1893-1904.

9 (a) K. V. Raman, A. M. Kamerbeek, A. Mukherjee, N. Atodiresei, T. K. Sen, P. Lazic, V. Caciuc, R. Michel, D. Stalke, S. K. Mandal, S. Blugel, M. Munzenberg and J. S. Moodera, *Nature*, 2013, **493**, 509-513; (b) A. Pariyar, G. Vijaykumar, M. Bhunia, S. K. Dey, S. K. Singh, S. Kurungot and S. K. Mandal, *J. Am. Chem. Soc.*, 2015, **137**, 5955-5960.

10 A. Mukherjee, S. C. Sau and S. K. Mandal, *Acc. Chem. Res.*, 2017, **50**, 1679−1691.

11 (a) *Comprehensive Handbook of Hydrosilylation*; Oxford, 1992; (b) V. B. Pukhnarevitch, E. Lukevics, L. I. Kopylova and M. Voronkov, *Perspectives of Hydrosilylation* (Institute for Organic Synthesis, Riga, Latvia, 1992).

12 (a) X. Chi, M. E. Itkis, B. O. Patrick, T. M. Barclay, R. W. Reed, R. T. Oakley, A. W. Cordes and R. C. Haddon, *J. Am. Chem. Soc.*, 1999, **121**, 10395–10402; (b) X. Chi, M. E. Itkis, K. Kirschbaum, A. A. Pinkerton, R. T. Oakley, A. W. Cordes and R. C. Haddon, *J. Am. Chem. Soc.*, 2001, **123**, 4041–4048; (c) S. K. Pal, M. E. Itkis, F. S. Tham, R. W. Reed, R. T. Oakley and R. C. Haddon *Science*, 2005, **309**, 281–284; (d) S. K. Mandal, M. E. Itkis, X. Chi, S. Samanta, D. Lidsky, R. W. Reed, R. T. Oakley, F. S. Tham and R. C. Haddon, *J. Am. Chem. Soc.*, 2005, **127**, 8185–8196.

13 (a) R. Paira, B. Singh, P. K. Hota, J. Ahmed, S. C. Sau, J. P. Johnpeter and S. K. Mandal, *J. Org. Chem.*, 2016, **81**, 2432–2441; (b) J. Ahmed, P. Sreejoythi, G. Vijaykumar, A. Jose, M. Raj and S. K. Mandal, *Chem. Sci.*, 2017, **8**, 7798–7806.

14 Y. Nakajima and S. Shimada, *RSC Adv.*, 2015, **5**, 20603-20616.

15 (a) M. F. Lappert, T. A. Nile and S. Takahashi, *J. Organometallic Chem.*, 1974, **72**, 425-439; (b) M. D. Greenhalgh, D. J. Frank and S. P. Thomas, *Adv. Synth. Catal.* 2014, **356**, 584−590; (c) K. Kamata, A. Suzuki, Y. Nakai and H. Nakazawa, *Organometallics,* 2012, **31**, 3825−3828; (d) V. Srinivas, Y. Nakajima, A. Wataru, S. Kazuhiko and S. Shigeru, *J. Organometallic Chem.*, 2016, **809**, 57-62; (e) K. Hayasaka, K. Kamata and H. Nakazawa, *Bull. Chem. Soc. Jpn.,* 2016, **89**, 394–404.

16 T. J. Steiman and C. Uyeda, *J. Am. Chem. Soc.,* 2015, **137**, 6104− 6110.

17 Ö. Metin, L. T. Yıldırım and S. Özkar, *Inorg. Chem. Commun.*, 2007, **10**, 1121-1123.

18 (a) P.-F. Fu, L. Brard, Y. Li and T. J. Marks, *J. Am. Chem. Soc.*, 1995, **117**, 7157-7168; (b) S. Anga, K. Naktode, H. Adimulam and T. K. Panda, *Dalton Trans.*, 2014, **43**, 14876–14888.

19 (a) L. Nielsen and T. Skrydstrup, *J. Am. Chem. Soc.*, 2008, **130**, 13145-13151; (b) I. Buslov, S. C. Keller and X. Hu, *Org. Lett.*, 2016, **18**, 1928-1931.

20 (a) J. L. Speier, J. A. Webster and G. H. Barnes, *J. Am. Chem. Soc.*, 1957, **79**, 974-979; (b) T. Galeandro-Diamant, M.-L. Zanota, R. Sayah, L. Veyre, C. Nikitine, C. de Bellefon, S. Marrot, V. Meille and C. Thieuleux, *Chem. Commun.*, 2015, **51**, 16194-16196.

21 P. Chaudhuri, C. N. Verani, E. Bill, E. Bothe, T. Weyhermüller and K. Wieghardt, *J. Am. Chem. Soc.*, 2001, **123**, 2213-2223.

22 C. C. Lu, E. Bill, T. Weyhermüller, E. Bothe and K. Wieghardt, *J. Am. Chem. Soc.*, 2008, **130**, 3181-3197.

23 A. Abragam and B. Bleaney, Electron Paramagnetic Resonance of Transition Ions, 1986.

24 (a) A. P. Clark and D. E. Wilcox, *Inorg. Chem.*, 1989, **28**, 1326; (b) H. R. Jiménez, J. Salgado, J. M. Moratal and I. Morgenstern-Badarau, *Inorg. Chem.*, 1996, **35**, 2737-2741.

25. J. Matienzo, L. I. Yin, S. O. Grim and W. E. Swartz, *Inorg. Chem.,* 1973, **12**, 2762-2769.

26 (a) L. Noodleman, *J. Chem. Phys.*, 1981, **74**, 5737-5743; (b) L. Noodleman and E. R. Davidson, *Chem. Phys.*, 1986, **109**, 131-143.

27 V. Bachler, G. Olbrich, F. Neese and K. Wieghardt, *Inorg. Chem.*, 2002, **41**, 4179-4193.

28 (a) R. L. Sweany and J. Halpern, *J. Am. Chem. Soc.,* 1977, **99**, 8335-8337; (b) J. Choi, L. Tang and J. R. Norton, *J. Am. Chem. Soc.*, 2007, **129**, 234-240; (c) S. W. M. Crossley, C. Obradors, R. M. Martinez and R. A. Shenvi, *Chem. Rev.*, 2016, **116**, 8912-9000.

29 (a) Z. Yang, M. Iqbal, A. R. Dobbie and J. G. C. Veinot, *J. Am. Chem. Soc.*, 2013, **135**, 17595-17601; (b) J. M. Buriak, *Chem. Mater.*, 2014, **26**, 763-772; (c) J. Navarro-Ruiz, A. Rimola and M. Sodupe, *J. Phys. Chem. C*, 2013, **117**, 15130-15138.

30 D. L. J. Broere, L. L. Metz, B. de Bruin, J. N. H. Reek, M. A. Siegler and J. I. van der Vlugt, *Angew. Chem., Int. Ed.*, 2015, **54**, 1516-1520.

31 A. J. Chalk and J. F. Harrod, *J. Am. Chem. Soc*., 1965, **87**, 16-21

32 (a) M. A. Schroeder and M. S. Wrighton, *J. Organomet. Chem*., 1977, **128**, 345−358; (b) J. C. Mitchener and M. S. Wrighton, *J. Am. Chem. Soc.,* 1981, **103**, 975−977.

33 I. Pappas, S. Treacy and P. J. Chirik, *ACS Catal.,* 2016, **6**, 4105− 4109.

34 R. C. Haddon, R. Rayford and A. M. Hirani, *J. Org. Chem.*, 1981, **46**, 4587-4588

35 M. J. Frisch, G. W. Trucks, H. B. Schlegel, G. E. Scuseria, M. A. Robb, J. R. Cheeseman, G. Scalmani, V. Barone, B. Mennucci, G. A. Petersson, et al. Gaussian 09, Gaussian Inc: Wallingford, CT, 2009.

36 O. V. Dolomanov, L. J. Bourhis, R. J. Gildea, J. A. K. Howard and H. Puschmann, OLEX2: a complete structure solution, refinement and analysis program. *J. Appl. Cryst.,* 2009, **42**, 339-341.

37 SUPERFLIP, *J. Appl. Cryst*. 2007, **40**, 786-790.

38 SHELXL, G. M. Sheldrick, *Acta Cryst*., 2008, **A64**, 112-122.

View Article Online
DOI: 10.1039/C7SC04687A

Hydrosilylation of olefins by nickel(II) catalyst assisted by a redox non-innocent phenalenyl (PLY) ligand. The ligand centred PLY radical initiates a SET process as the first step of such catalysis.